

**Imprint of transition metal  $d$  orbitals on a graphene Dirac cone**

Qin Zhou, Sinisa Coh, Marvin L. Cohen, Steven G. Louie, and A. Zettl

*Department of Physics, University of California at Berkeley, Berkeley, California 94720, USA  
and Materials Sciences Division, Lawrence Berkeley National Laboratory, Berkeley, California 94720, USA*

(Received 28 June 2013; published 23 December 2013)

We investigate the influence of SiO<sub>2</sub>, Au, Ag, Cu, and Pt substrates on the Raman spectrum of graphene. Experiments reveal particularly strong modifications to the Raman signal of graphene on platinum, compared to that of suspended graphene. The modifications strongly depend on the relative orientation of the graphene and platinum lattices. These observations are theoretically investigated and shown to originate basically from hybridization of electronic states in graphene and  $d$  orbitals in platinum. It is expected that, quite generally, hybridization between graphene and any material with  $d$  orbitals near the Fermi level will result in an imprint on the graphene Dirac cone, which depends sensitively on the relative orientation of the respective lattices.

DOI: [10.1103/PhysRevB.88.235431](https://doi.org/10.1103/PhysRevB.88.235431)

PACS number(s): 73.22.Pr, 78.67.Wj, 78.30.Na

**I. INTRODUCTION**

Raman spectroscopy has proven to be particularly useful in elucidating the vibrational phonon structure of low-dimensional solids such as fullerenes, nanotubes, and graphene.<sup>1-7</sup> In graphene, Raman also serves as a convenient, relatively local ( $\sim 1 \mu\text{m}$  size scale) probe of sample layer number and defect concentration for exfoliated samples or those grown directly on metal substrates such as Cu. Recently there has been success in growing relatively flat and large-grain-size, high-quality graphene on platinum.<sup>8-10</sup> Interestingly, the Raman signal from graphene on Pt can be orders of magnitude smaller in intensity than that from graphene on Cu or SiO<sub>2</sub>. This result, surprising in light of the assumed weak van der Waals interaction between graphene and Pt,<sup>8,10-13</sup> has been vaguely attributed to an unspecified “strong platinum-graphene interaction”.<sup>9,14</sup> Proper identification and understanding of the suppression mechanism is lacking.

We here contrast the Raman signature of suspended graphene, graphene on SiO<sub>2</sub>, Au, Ag, Cu, and Pt, including single-crystal Pt, and floated graphene brought close to a Pt surface. The results for Pt cannot be accounted for by simple substrate screening. Instead, our experiments and theoretical investigation reveal rich physics underlying the Raman spectrum modification. For graphene on Pt, the Raman spectrum reflects the hybridization between graphene Dirac cone states and Pt  $d$  orbitals, where the hybridization is strongly dependent on the in-plane position of the  $d$  orbital relative to the graphene lattice, and on the orbital character. The  $s$  orbitals interact very weakly with the Dirac cone because of the specific nature of the graphene band structure. Thus, and rather remarkably, Raman spectroscopy reveals a detailed imprint of the transition metal  $d$  orbitals on the Dirac cone. The  $d$  orbitals in Au, Ag, and Cu are too far from the Fermi level (more than 2 eV below) to affect the Raman signal in our experiment.

**II. EXPERIMENT**

Graphene samples used in this work are prepared by chemical vapor deposition (CVD),<sup>8,9,15</sup> either grown directly on the substrate of interest [Cu or Pt polycrystalline foils, or Pt(111) single crystal] or transferred post growth from Cu or

Pt onto SiO<sub>2</sub> (1-mm-thick fused silica), Au, Ag, and selected Pt substrates. The suspended graphene sample is prepared following our previous work.<sup>16</sup> Graphene is removed from Cu via conventional etching<sup>15</sup> and from Pt via bubble release.<sup>8</sup> Raman measurements are performed primarily using a laser wavelength of 488 or 514 nm and power 0.9 mW. Details of the sample preparation can be found in the Supplemental Material.<sup>17</sup>

Figure 1 shows details of the Raman spectrum measured by a 514 nm laser near 2600 cm<sup>-1</sup> [2D peak] and 1600 cm<sup>-1</sup> ( $G$  peak) of suspended graphene and graphene on various substrates. The spectra for graphene transferred onto SiO<sub>2</sub>, Au, or Ag substrates have reduced intensity, but the 2D and  $G$  peak positions, width, and 2D/ $G$  intensity ratios are similar to those for suspended graphene. The spectrum of graphene grown directly on Cu shows blueshifted  $G$  and 2D peaks, indicating compressive strain,<sup>18</sup> as previously reported. The spectrum of graphene grown on Pt has dramatically reduced and sometimes substantially shifted 2D and  $G$  peaks. The peaks can vary significantly from place to place, producing location-dependent results (however, if only one location of the sample is measured, the result is highly consistent). Figure 1 shows one example, where the 2D peak for graphene on Pt is nearly four orders of magnitude smaller than that for suspended graphene, and blueshifted by over 50 cm<sup>-1</sup>. The  $G$  peak for the same sample region is reduced by nearly two orders of magnitude. We have also prepared a sample of graphene floated on water, where the graphene is brought close to a bare Pt surface by evaporating the water. The graphene Raman signal is high (and reminiscent of suspended graphene) with a water spacer present, but is largely quenched when the graphene touches the Pt (data in Supplemental Material<sup>17</sup>).

**III. RESULTS AND DISCUSSION**

We first explore electromagnetic screening as a possible cause for the quenching of the Raman signal of graphene on Pt. Electromagnetic screening arises from reduced optical fields from electromagnetic antiresonances in the substrates.<sup>19</sup> To a first approximation, the screening factor  $S$  can be expressed by the fourth power of the ratio of the total electric field  $E_s$  at the graphene location to the incident excitation field  $E_{in}$ .<sup>20</sup>

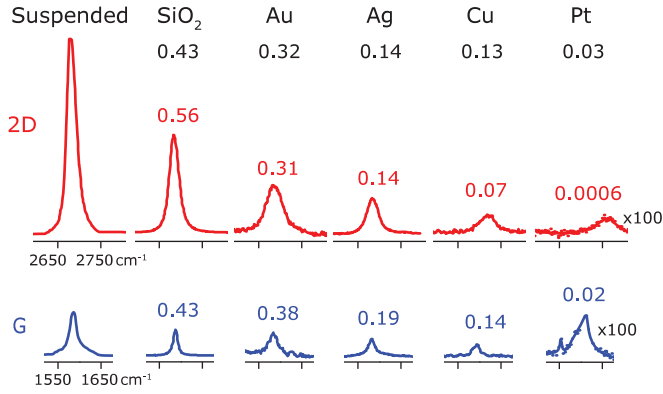


FIG. 1. (Color online) The Raman signal for graphene on platinum is strongly suppressed compared to suspended graphene, and graphene on SiO<sub>2</sub>, Au, Ag, and Cu (514 nm laser, 10 s integration). The data on Pt are from 5000 s integration time and amplified by 100 times for better viewing. The small peak at  $\sim 1554 \text{ cm}^{-1}$  near the G peak on Pt is from environment oxygen.<sup>38</sup> The numbers (black) below the substrate labels are the predicted peak intensity based only on screening [Eq. (1)]. The numbers above each curve are the experimentally measured peak intensities. The intensity is defined as the area covered by the peak and all the intensity values are normalized to the ones from suspended graphene.

Employing the Fresnel equations yields

$$S = \left| \frac{\mathbf{E}_s}{\mathbf{E}_{in}} \right|^4 = \left| \frac{\mathbf{E}_{in} + \mathbf{E}_r}{\mathbf{E}_{in}} \right|^4 = \left| 1 + \frac{1-n}{1+n} \right|^4 = \left| \frac{2}{1+n} \right|^4, \quad (1)$$

where  $n$  is the complex refractive index of the substrate.<sup>21</sup> Equation (1) predicts  $S$  values of 0.43, 0.32, 0.14, 0.13, and 0.03 for SiO<sub>2</sub>, Au, Ag, Cu, and Pt substrates, respectively. These values are shown in Fig. 1 in black below the respective substrate along with the experimentally derived peak intensities (all normalized to suspended graphene). The observed peak intensities for SiO<sub>2</sub>, Au, Ag, and Cu substrates can be reasonably well accounted for by screening, but the 2D peak for graphene on Pt is approximately 50 times smaller than expected. Indeed, as we show below, under certain circumstances the 2D peak for graphene on Pt can be virtually

undetectable. Hence screening is eliminated as the sole cause of Raman signal quenching for graphene on Pt.

We next consider Pauli blocking as a cause of the Raman signal quenching. The G and 2D peaks of graphene result from resonance Raman processes, in which electrons are first excited to the conduction band by the incoming photons and then interact with phonons. Given the large work function difference between graphene and platinum (4.48 and 6.13 eV, respectively<sup>22</sup>), graphene could transfer significant charge to Pt, resulting in the electron excitation being Pauli blocked. However, both theory and experiment indicate a relatively small Fermi level shift of  $\sim 0.4 \text{ eV}$  relative to the Dirac point.<sup>10,22,23</sup> This energy shift is not sufficient to block the optical transition caused by photons with energy up to 2.5 eV (488 nm). We also note that doping or strain could shift the peak position,<sup>24,25</sup> but they have little effect on intensities and peak widths.

#### IV. MODELING AND CALCULATION OF HYBRIDIZATION

Therefore, we turn to more in-depth theoretical calculations to clarify the reduction of the Raman 2D signal in graphene on Pt. Figure 2 shows our band structure calculation<sup>26,27</sup> of graphene on a Pt slab. The distance between the graphene and the platinum slab is kept at  $z = 3.3 \text{ \AA}$ ,<sup>10,28</sup> and we consider the three most common relative orientations of the graphene lattice with respect to the Pt(111) surface.<sup>29</sup> The Dirac cone is strongly hybridized when in contact with the Pt slab. Furthermore, the size and the orbital character (different colors in Fig. 2) of the hybridization gap depend strongly on the relative orientation of the graphene lattice with respect to the Pt lattice (compare orientations  $\alpha$ ,  $\beta$ , and  $\gamma$ <sup>29</sup> in Fig. 2).

From Fig. 2, it is clear that the effect of the Pt hybridization with the graphene Dirac cone is quite complicated. We first work with a simplified model in which graphene states are hybridized with only one metallic ( $s$  or  $d$ ) orbital per graphene unit cell, and vary the metallic orbital position and character. Furthermore, we assume that these metallic orbitals form a flat energy band, so that we can easily tune their energy relative to the Dirac point. We parameterize the hybridization strength

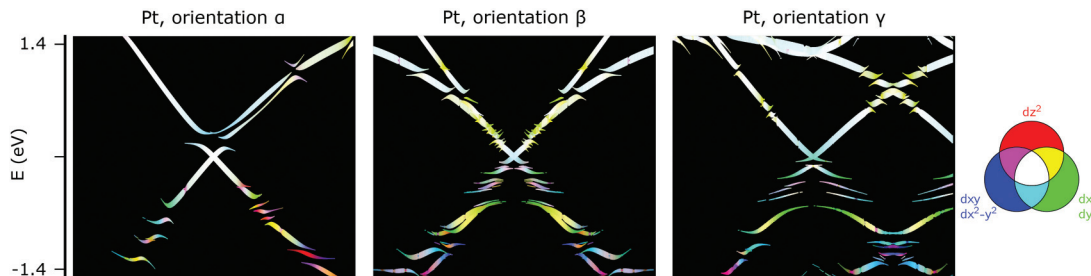


FIG. 2. (Color online) The graphene Dirac cone is strongly affected by a Pt substrate, and varies substantially between the three most common misorientations of the graphene and Pt lattices (orientations  $\alpha$ ,  $\beta$ , and  $\gamma$ <sup>29</sup> correspond to  $2 \times 2$ ,  $3 \times 3$ , and  $4 \times 4$  graphene lattice supercells). A comparison of the Au substrate where the cone structure is preserved in this energy range can be found in Supplemental Material.<sup>17</sup> The thickness of each line in the plot is proportional to the graphenelike character of the state. The color of each line segment is proportional to the mixture of graphene states with different metallic  $d$  orbitals in the topmost layer of the Pt slab substrate. Red, green, and blue color components correspond to three different projections of the angular momentum perpendicular to the platinum surface ( $m = 0, +1 - 1$ , or  $+1 - 2$ , respectively). Graphene states with no  $d$  character are colored white. The path in reciprocal space for all three misorientations is along the  $\Gamma$ - $K$ - $M$  line of the primitive graphene Brillouin zone.

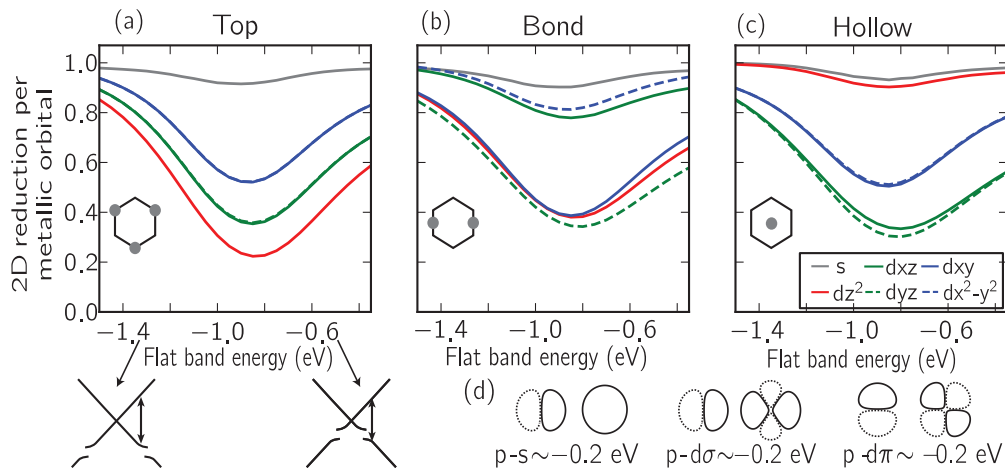


FIG. 3. (Color online) Reduction of the graphene Raman (laser energy: 1.96 eV) 2D signal intensity upon hybridization with a metallic flat band (with only one metallic orbital per graphene unit cell). (a) – (c) Reduction of the Raman 2D signal depending on the position of the metallic orbital with respect to the graphene lattice (different panels), orbital character (different line colors and styles), and energy of the metallic band relative to the Dirac cone (horizontal axis). Reduction of the Raman 2D signal is almost negligible for the  $s$  orbital, even though its head-to-head matrix element is of the same order of magnitude as for the  $d$  orbital [both in  $\sigma$  and  $\pi$  orientation; see (d)]. The effect of  $d$  orbital hybridization is strongly dependent on the  $d$  orbital character.

between the graphene  $p_z$  orbitals and the metallic  $s$  and  $d$  orbitals using the full density-functional-theory calculation (see Supplemental Material<sup>17</sup>). This yields the hybridization matrix element between carbon  $p_z$  and Pt orbitals at the same in-plane position (head to head), but separated vertically by  $z$ . It is close to  $-0.2$  eV for both  $s$  and  $d$  orbitals [see Fig. 3(d)], but as the in-plane separation between the carbon  $p_z$  and metallic orbitals is increased, hybridization with strongly anisotropic  $d$  orbitals results in a much faster decay than with the isotropic  $s$  orbitals. In this simplified model, an almost negligible hybridization gap is opened by the metallic  $s$  orbitals, while the size of the hybridization gap opened by the metallic  $d$  orbitals is strongly dependent on the orbital  $d$  character and position relative to the graphene lattice. These observations are consistent with those from the calculations shown in Fig. 2, and with previous work.<sup>30–33</sup>

Next we compute the graphene Raman  $G$  and 2D signals using a simplified model following Ref. 34. We neglect the effects of the metallic slab on the graphene phonon frequencies and focus only on the electronic state modifications. Our Raman calculation shows that the hybridization of graphene states with metal orbitals reduces the Raman 2D signal and that this reduction is a direct measure of the hybridization gap size. Furthermore, hybridization also shifts the Raman 2D peak position, increases its width, and introduces new Raman peak substructure (see Supplemental Material<sup>17</sup>). Figure 3 shows the dependence of the Raman 2D signal reduction on the orbital position. Comparing the effect of  $s$  and  $d$  orbitals on the 2D signal reduction, we find that  $s$  orbitals have an almost negligible effect. Additionally, the effect of  $d$  orbitals is strongly dependent on both  $d$  orbital position and orbital character. Finally, the Raman 2D signal reduction is maximal when the hybridization gap is well matched with the energy of the incoming photons.

Figure 3 shows that *one* metallic  $d$  orbital per graphene unit cell reduces the Raman 2D intensity at most by a factor of four.

Taking into account a more realistic number of  $d$  orbitals per graphene unit cell ( $\sim 5$ ) and repeating our model calculation for this case, we find that the 2D intensity of graphene on platinum can be reduced up to 20 times. As in the case of one metallic  $d$  orbital per graphene cell, total 2D intensity reduction with multiple  $d$  orbitals per cell is in a one-to-one relation with the total hybridization gap size.

Unlike the case for the Raman 2D signal, we find almost no influence of hybridization on the Raman  $G$  signal intensity. This can be explained by considering the different origin of the Raman  $G$  signal compared to the 2D signal.<sup>34</sup> The Raman  $G$  signal intensity even in suspended graphene is severely reduced in intensity because of the coherent cancellation between amplitudes of various electron-hole pairs in the Dirac cone. In fact, a perfectly linear Dirac cone dispersion leads to a Raman  $G$  signal with vanishing intensity. Therefore, any small imperfections in the band structure (such as trigonal warping) will lead to an incomplete cancellation of the Raman amplitudes, and will thus produce a measurable Raman  $G$  signal. This observation also explains why we find a small *increase* in the calculated Raman  $G$  signal intensity upon hybridization with metallic orbitals (see Supplemental Material<sup>17</sup>), as hybridization with metallic orbitals leads to a more incomplete cancellation of the  $G$  signal amplitudes.

## V. EXPERIMENTAL VERIFICATION

Our theoretical analysis predicts that the Raman 2D (but not  $G$ ) peak of graphene on Pt will be highly dependent on the relative orientation between the graphene and Pt lattices. To experimentally obtain a range of different lattice orientations, we grow large-area graphene on a polycrystalline platinum foil. We also grow single-domain graphene on single-crystal Pt(111).

Figure 4 shows graphene Raman spectra measured at different locations on the polycrystalline Pt substrate and the

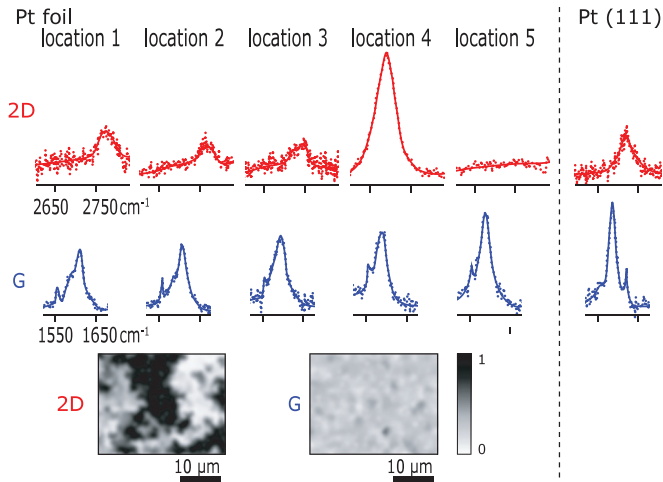


FIG. 4. (Color online) Left: Raman spectra of graphene measured at different locations on a polycrystalline Pt foil. Laser wavelength: 488 nm. The intensity maps of a  $30 \times 25 \mu\text{m}$  region are shown at the bottom. Right: Raman spectra for graphene on single-crystal Pt(111) with  $2 \times 2$  graphene supercell (also shown in Fig. 2). In this case, the intensity for both the 2D and G peaks is found to be uniform across the single-domain sample.

single-crystal Pt substrate (we switch to a 488 nm laser here because it has weaker metallic screening and can therefore measure Raman spectra more efficiently. Data for other laser wavelengths can be found in the Supplemental Material<sup>17</sup>). For the polycrystalline substrate, a small variable shift of the position of the G peak (from 0 to  $25 \text{ cm}^{-1}$ ) is found, with nearly constant intensity, in agreement with the theoretical discussion above. The small shift of the G peak likely originates from an inhomogeneous strain field developed during the cooling process<sup>35,36</sup> after graphene synthesis. On the other hand, the intensity, width, position, and shape of the Raman 2D peak vary strongly at different sample positions. The position of the 2D peak can shift anywhere between  $-8$  and  $100 \text{ cm}^{-1}$  with respect to the suspended graphene. In many cases, the inhomogeneous shift is too large to be accounted solely by strain or doping,<sup>18,29</sup> and is therefore an indication of orbital hybridization according to our theory. The width of the 2D peak is between  $25$  and  $65 \text{ cm}^{-1}$ , and it likely contains multiple components. The 2D peak intensity is reduced between 2.6 and 40 times on top of the reduction coming solely from the metallic screening (reduction factor  $S = 1/29$ ), yielding a total reduction between 75 and 1100 times, consistent with the total reductions predicted by our hybridization model including metallic screening. Typical location-dependent reductions are illustrated in the first four curves in Fig. 4. Interestingly, at a few locations (less than 10% of the sample surface) for polycrystalline substrate samples, the Raman 2D peak appears

entirely unobservable. A prolonged 10 000 s integration is performed at one such spot (Fig. 4, fifth curve) which suggests, for these rare locations, a total reduction of more than 10 000.<sup>37</sup> Such extreme reductions may necessitate a model beyond a simplified flat band one. Unfortunately, the interface between graphene and polycrystalline Pt can be rather complicated due to the unknown exposed crystalline plane and surface reconstruction of Pt for experimental and theoretical characterization. We note that an extreme reduction of the Raman signal is never observed for graphene on single-crystalline Pt(111) (Fig. 4, right panel).

The lower insets to Fig. 4 display the degree of spatial inhomogeneity for the G and 2D peak for graphene on Pt. The intensity of the G peak is relatively insensitive to position (i.e., lattice misorientation), while the intensity map of the 2D peak reflects directly the regions of different lattice misorientation. For single-domain graphene on single-crystal Pt(111) with the consistent  $2 \times 2$  supercell structure, both the G and 2D peak intensities are homogeneous, as expected.

## VI. SUMMARY

In conclusion, we observed strong location-dependent suppression and modulation of the graphene Raman signal when in contact with platinum. We assign this observation to electronic hybridization between graphene Dirac cone states and platinum *d* orbitals. The hybridization is strongly dependent on the metal orbital character, which can be used for tuning the graphene Dirac cone.

## ACKNOWLEDGMENTS

This research was supported in part by the *sp*<sup>2</sup>-bonded Materials Program of the Lawrence Berkeley National Laboratory funded by the Director, Office of Energy Research, Office of Basic Energy Sciences, Materials Sciences and Engineering Division, of the U.S. Department of Energy under Contract No. DE-AC02-05CH11231 which provided for Raman spectroscopy, theoretical Raman intensity analysis and calculations, and postdoctoral assistance; by the National Science Foundation under Grant No. DMR-1206512 which provided for graphene transfer and structural characterization; by the National Science Foundation under Grant No. DMR-10-1006184 which provided *ab initio* band structure study; and by the U.S. Office of Naval Research under Grant No. N00014-12-1-1008 which provided for graphene growth. Computational resources have been provided by the U.S. Department of Energy at Lawrence Berkeley National Laboratory's NERSC facility. We thank C. Hwang for help with ARPES measurements, A. T. N'Diaye for help with LEED measurements, and H. Rasool for technical assistance. S.G.L. acknowledges the support of a Simons Foundation Fellowship in Theoretical Physics.

<sup>1</sup>L. Malard, M. Pimenta, G. Dresselhaus, and M. Dresselhaus, *Phys. Rep.* **473**, 51 (2009).

<sup>2</sup>A. C. Ferrari, *Solid State Commun.* **143**, 47 (2007).

<sup>3</sup>A. C. Ferrari, J. C. Meyer, V. Scardaci, C. Casiraghi, M. Lazzeri, F. Mauri, S. Piscanec, D. Jiang, K. S. Novoselov, S. Roth, and A. K. Geim, *Phys. Rev. Lett.* **97**, 187401 (2006).

- <sup>4</sup>M. Dresselhaus, G. Dresselhaus, and P. Eklund, *J. Raman Spectrosc.* **27**, 351 (1996).
- <sup>5</sup>A. Rao, E. Richter, S. Bandow, B. Chase, P. Eklund, K. Williams, S. Fang, K. Subbaswamy, M. Menon, and A. Thess, *Science* **275**, 187 (1997).
- <sup>6</sup>A. Jorio, R. Saito, J. H. Hafner, C. M. Lieber, M. Hunter, T. McClure, G. Dresselhaus, and M. S. Dresselhaus, *Phys. Rev. Lett.* **86**, 1118 (2001).
- <sup>7</sup>M. S. Dresselhaus, G. Dresselhaus, R. Saito, and A. Jorio, *Phys. Rep.* **409**, 47 (2005).
- <sup>8</sup>L. B. Gao, W. C. Ren, H. L. Xu, L. Jin, Z. X. Wang, T. Ma, L. P. Ma, Z. Y. Zhang, Q. Fu, L. M. Peng, X. H. Bao, and H. M. Cheng, *Nat. Commun.* **3**, 699 (2012).
- <sup>9</sup>B. J. Kang, J. H. Mun, C. Y. Hwang, and B. J. Cho, *J. Appl. Phys.* **106**, 104309 (2009).
- <sup>10</sup>P. Sutter, J. T. Sadowski, and E. Sutter, *Phys. Rev. B* **80**, 245411 (2009).
- <sup>11</sup>A. B. Preobrajenski, M. L. Ng, A. S. Vinogradov, and N. Martensson, *Phys. Rev. B* **78**, 073401 (2008).
- <sup>12</sup>M. Gao, Y. Pan, L. Huang, H. Hu, L. Z. Zhang, H. M. Guo, S. X. Du, and H. J. Gao, *Appl. Phys. Lett.* **98**, 033101 (2011).
- <sup>13</sup>M. Gao, Y. Pan, C. D. Zhang, H. Hu, R. Yang, H. L. Lu, J. M. Cai, S. X. Du, F. Liu, and H. J. Gao, *Appl. Phys. Lett.* **96**, 053109 (2010).
- <sup>14</sup>J.-H. Gao, K. Sagisaka, M. Kitahara, M.-S. Xu, S. Miyamoto, and D. Fujita, *Nanotechnology* **23**, 055704 (2012).
- <sup>15</sup>X. Li, W. Cai, J. An, S. Kim, J. Nah, D. Yang, R. Piner, A. Velamakanni, I. Jung, and E. Tutuc, *Science* **324**, 1312 (2009).
- <sup>16</sup>W. Regan, N. Alem, B. Alemán, B. Geng, C. Girit, L. Maserati, F. Wang, M. Crommie, and A. Zettl, *Appl. Phys. Lett.* **96**, 113102 (2010).
- <sup>17</sup>See Supplemental Material at <http://link.aps.org/supplemental/10.1103/PhysRevB.88.235431> for more details in graphene growth, graphene transfer, and Raman measurement.
- <sup>18</sup>J. E. Lee, G. Ahn, J. Shim, Y. S. Lee, and S. Ryu, *Nat. Commun.* **3**, 1024 (2012).
- <sup>19</sup>K. Kneipp, Y. Wang, H. Kneipp, L. T. Perelman, I. Itzkan, R. R. Dasari, and M. S. Feld, *Phys. Rev. Lett.* **78**, 1667 (1997).
- <sup>20</sup>F. J. Garcia-Vidal, and J. B. Pendry, *Phys. Rev. Lett.* **77**, 1163 (1996).
- <sup>21</sup>E. D. Palik, and G. Ghosh, *Handbook of Optical Constants of Solids* (Academic, San Diego, 1998).
- <sup>22</sup>G. Giovannetti, P. A. Khomyakov, G. Brocks, V. M. Karpan, J. van den Brink, and P. J. Kelly, *Phys. Rev. Lett.* **101**, 026803 (2008).
- <sup>23</sup>P. A. Khomyakov, G. Giovannetti, P. C. Rusu, G. Brocks, J. van den Brink, and P. J. Kelly, *Phys. Rev. B* **79**, 195425 (2009).
- <sup>24</sup>M. Huang, H. Yan, C. Chen, D. Song, T. F. Heinz, and J. Hone, *Proc. Natl. Acad. Sci. USA* **106**, 7304 (2009).
- <sup>25</sup>T. M. G. Mohiuddin, A. Lombardo, R. R. Nair, A. Bonetti, G. Savini, R. Jalil, N. Bonini, D. M. Basko, C. Galiotis, N. Marzari, K. S. Novoselov, A. K. Geim, and A. C. Ferrari, *Phys. Rev. B* **79**, 205433 (2009).
- <sup>26</sup>P. Giannozzi, S. Baroni, N. Bonini, M. Calandra, R. Car, C. Cavazzoni, D. Ceresoli, G. L. Chiarotti, M. Cococcioni, and I. Dabo, *J. Phys.: Condens. Matter* **21**, 395502 (2009).
- <sup>27</sup>J. P. Perdew, K. Burke, and M. Ernzerhof, *Phys. Rev. Lett.* **77**, 3865 (1996).
- <sup>28</sup>I. Hamada, and M. Otani, *Phys. Rev. B* **82**, 153412 (2010).
- <sup>29</sup>P. Merino, M. Svec, A. L. Pinardi, G. Otero, and J. A. Martin-Gago, *ACS Nano* **5**, 5627 (2011).
- <sup>30</sup>T. O. Wehling, H. P. Dahal, A. I. Lichtenstein, M. I. Katsnelson, H. C. Manoharan, and A. V. Balatsky, *Phys. Rev. B* **81**, 085413 (2010).
- <sup>31</sup>M. Gyamfi, T. Eelbo, M. Waśniowska, T. O. Wehling, S. Forti, U. Starke, A. I. Lichtenstein, M. I. Katsnelson, and R. Wiesendanger, *Phys. Rev. B* **85**, 161406(R) (2012).
- <sup>32</sup>T. O. Wehling, A. V. Balatsky, M. I. Katsnelson, A. I. Lichtenstein, and A. Rosch, *Phys. Rev. B* **81**, 115427 (2010).
- <sup>33</sup>D. Jacob, and G. Kotliar, *Phys. Rev. B* **82**, 085423 (2010).
- <sup>34</sup>S. Coh, L. Z. Tan, S. G. Louie, and M. L. Cohen, *Phys. Rev. B* **88**, 165431 (2013).
- <sup>35</sup>Y. F. Zhang, T. Gao, Y. B. Gao, S. B. Xie, Q. Q. Ji, K. Yan, H. L. Peng, and Z. F. Liu, *ACS Nano* **5**, 4014 (2011).
- <sup>36</sup>N. Ferralis, *J. Mater. Sci.* **45**, 5135 (2010).
- <sup>37</sup>The vanishing of the 2D peak is also laser frequency dependent. At sample locations where the 2D peak intensity is virtually undetectable at one laser energy (e.g., 633 nm laser), it is observable at another laser energy (e.g., 514 nm laser). See Sec. V of Supplemental Material (Ref. 17).
- <sup>38</sup>J. B. Dunn, D. F. Shriver, and I. M. Klotz, *Proc. Natl. Acad. Sci. USA* **70**, 2582 (1973).